# Simple and convenient measurement of RBC deformability using QCM integrated with a novel model of cell viscoelasticity

**Authors:**

Vitaly Efremov[1], Ramji S. Lakshmanan[1], Barry Byrne[1] and Anthony J. Killard[1,2]

**Affiliations:**

[1] Biomedical Diagnostics Institute, Dublin City University, Dublin 9, Ireland.

[2] Department of Applied Sciences, Faculty of Health and Applied Sciences, University of the West of England, Coldharbour Lane, Bristol BS16 1QY, UK.

**Abstract**

It is well-established that alterations in cell morphology are regulated by cell signalling pathways, with the qualitative and quantitative monitoring of these intrinsic processes being of potential diagnostic value. Moreover, the deformability of red blood cells (RBCs) plays a key role in microcirculation, with alterations in rigidity correlated with disease models such as diabetes mellitus, sickle cell anaemia and sepsis. Here a novel assay for monitoring changes in deformability of RBCs is described that integrates quartz-crystal microbalance and a mathematical model, and extrapolates qualitative and quantitative information pertinent to changes in cell elasticity. The ability of this assay to differentiate reliably between normal RBCs and ones artificially rigidized in a manner consistent with the disease-state RBCs is demonstrated. This simple, benchtop assay has significant potential for application in disease cohorts where aberrant deformability of RBCs is indicative of disease progression.

**Keywords**

Quartz Crystal Microbalance, Elasticity, Viscoelasticity, Rigidity, Deformability, RBC, Red Blood Cell

## 1. Introduction

The deformability potential of RBCs plays a significant role in the microcirculation, where the dimensions of the individual cells correlate with those of the surrounding blood vessels [1]. However, alterations in deformability and conversely, the rigidity of RBCs is also intrinsically-linked with disease progression in models such as sepsis [2, 3], sickle cell anaemia [4, 5] and malaria [6]. Furthermore, RBC deformability is one of several rheological parameters altered during the onset of diabetes mellitus [7, 8]. Convenient and accessible methods for measuring RBC deformability could prove extremely useful for research in areas such as sepsis and sickle cell disease. Of particular potential is the use of RBC deformability as a pre-symptomatic indicator of microangiopathy, which is s serious symptom of diabetes, which results in retinopathy, nephropathy and peripheral artery disease. It may also allow the effectiveness of treatment to be determined by monitoring changes in deformability over time as RBCs have a lifespan of 120 days. Such methods could be extended to point-of-care use in GP surgeries if appropriate technology was available.

Techniques for measuring RBC deformability have been reviewed [9, 10] and include micropipettes [11], atomic force microscopy (AFM) [12, 13] optical tweezers [14] and quantitative phase imaging (QPI) [15] for measuring individual cells and filtration [16], microfluidic filtration [17], and laser diffractometry (ektacytometry) [18] for measuring populations of cells. Cell deformability is a complex measurement and all these techniques probe different characteristics and measure different aspects of RBC deformability and remain largely experimental. While ektacytometry is the most widely used technique due to its precision, sensitivity, convenience and availability as an established commercial technology, it is a complex and time-consuming optical instrumental approach. Convenient and routine measurement of RBC deformability remains a challenge and a limitation in clinical application.

Quartz crystal microbalance (QCM) permits the monitoring of changes in the mechanical properties of cells coupled with its surface through the measurement of changes in resonant frequency ($\Delta f(t) = f(t)-f_{air}$) as well as in "dissipation" parameters such as resonant peak half-width-at-half-max ($\Delta\Gamma(t) = \Gamma(t)-\Gamma_{air}$) [19-21]. Analysis of the raw data set $\{\Delta f, \Delta\Gamma\}$ is often sufficient to identify an effect and obtain some qualitative conclusions, but is not enough for the development of robust diagnostic algorithms, since a "dose-effect" curve can be non-linear and ambiguous. However, the information hidden in $\{\Delta f, \Delta\Gamma\}$ can be extracted with the application of an properly selected mathematical model. This often allows problem linearization and meaningful data interpretation [21-23]. In this work, a novel assay is described which integrates standard QCM measurement with a mathematical model which extrapolates quantitative information pertinent to changes in RBC elasticity in an unambiguous manner.

## 2. Methods

Normal healthy volunteers were recruited at Dublin City University, and venous blood was collected from the antecubital vein with minimum stasis, and was citrated to provide a final sodium citrate concentration of 10.5 mmol/L. Blood was stored at 37°C for a period not longer than 1 hour post-collection. RBC cell suspensions were prepared with centrifugation of blood at 200xg for 10 min, followed by platelet rich plasma extraction and RBC cell culture dilution in phosphate buffered saline (PBS, 1:10 and 1:100 v/v dilutions). RBCs were artificially rigidized by incubation at room temperature for 20 minutes in the presence of 0.05% (v/v) glutaraldehyde (GA) [24]. According to [24], such concentration of GA provides 3-4 fold increase of of RBC membrane elasticity which corresponds to 'sickle cell trait' conditions with a shift in Young's modulus from approximately 1 kPa to 3-4 kPa [25].

QCM sensors, manufactured by Maxtek Inc. (Torrance, CA, U.S.), were used. The power supply conditions were selected to obtain optimal spectral characteristics of motional impedance close to a first mode frequency of 5 MHz. An Agilent 4395A (Agilent Technologies, Santa Clara, CA, U.S.) spectrum analyser was used with a minimal scanning frequency step of 0.1 Hz. Data acquisition was performed using a custom-developed LabView (version 2010) interface with the maximal time step of 1.5 s. Resonance curves were fitted by a rational function approximation algorithm [26] to evaluate resonant frequency $f$ and peak half-bandwidth $\Gamma$. Unloaded sensor surfaces demonstrated high-quality characteristics of approximately $f_{air} \approx 5\ MHz$ and $\Gamma_{air} < 30\ Hz$ .

A PMMA cylindrical QCM holding chamber (total volume ≈300 µl) was designed in order to perform insulated. leak-free fluidic sample contact with the QCM surface and fast fluid replacement in the chamber. Both QCM sensor and all fluidic elements of the experimental setup were kept at 37°C for 30 minutes before and during the test. Fig. 1 illustrates the experimental design with the recording of $\{\Delta f, \Delta\Gamma\}$ over time. The sample chamber is first filled with PBS whereupon a symmetric Newtonian fluid type response is observed ($-\Delta f \approx \Delta\Gamma$), which is then replaced by poly-L-lysine (PLL) solution (0.1%, w/v in PBS) for 6 minutes. The effect of PLL rigid mass layer formation on the bare gold QCM surface can be observed by the shift of $f$ with no change in $\Gamma$. Finally, the PLL solution is washed from the chamber with PBS, and the test RBC suspension (1:10 dilution in this example) is introduced for 20 minutes. During this phase the RBCs are captured by the positively charged PLL layer and accumulate on the sensor surface. The sensor response here is not symmetrical ($-d\Delta f \neq d\Delta\Gamma$) indicating a non-Newtonian fluid [21, 23]. Moreover one can see a significant difference in raw data between suspensions of normal and rigidized cells (taken initially from the same donor). The interpretation of the raw data does not appear obvious. The mathematical model adapted for blood component viscoelasticity analysis (developed earlier, see [23]) was applied. The model considers each individual cell as a “mass-spring” unit being surrounded by Newtonian fluid, the viscosity of which does not change during the experiment, and for which only cells directly captured by the surface have an impact on $\Delta f$ and $\Delta\Gamma$ values (Fig. 2). It would also be important to mention that the penetration depth of QCM oscillations in water/buffer/plasma is not deeper than 250 nm [27], and hence, only a single layer of adhered cells is measurable.

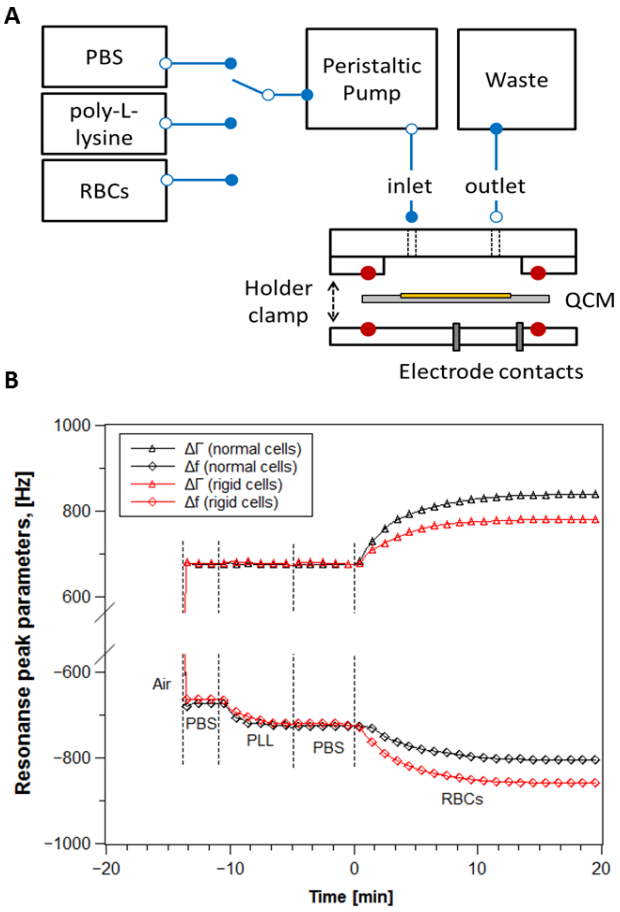


**Fig.1.** The RBC deformability experiment: a- setup schematics; b – recorded time courses. RBCs are coupled to the QCM surface using poly-L-lysine (PLL).

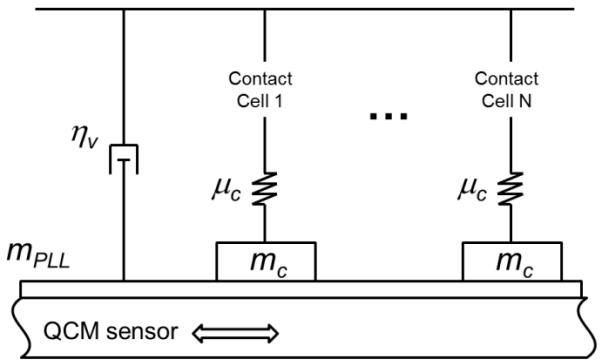


**Fig. 2.** Mechanical representation of the mathematical model.

The model assumes that each individual cell consists of two layers, namely contact rigid layer and bulk elastic layer. The contact rigid layer, characterised by a parameter of mass density, $m_c$, is the part of a cell which is firmly coupled to the sensor surface and hence not dissipating the energy of oscillations. The bulk elastic layer, characterised by a parameter of elasticity, $\mu_c$, is the part of a cell that oscillates not in phase with the surface and hence dissipates the energy. Derivation of the equations and detailed analysis of the model can be found in [23]. In short, the model derivation is based on a known concept of complex frequency and small load approximations [28]. In a general case of a rigid mass layer with a semi-infinite viscoelastic layer on top of it, the equation for the complex resonant frequency can be written as follows:

$$\Delta f(t) + j\Delta\Gamma(t) = C(j\rho^{\frac{1}{2}}G^{\frac{1}{2}} - 2\pi f_{air}EMD) \quad (1)$$

where *C* is a coefficient characterising QCM sensitivity depending on temperature, the type of sensor, power supply etc., but which does not change during the test. *EMD* is the effective mass density of the rigid mass layer. $\rho$ and *G* are viscoelastic layer density and complex shear modulus, respectively. For the particular circuit diagram shown in Fig.2, the rigid mass layer is formed by the PLL layer and the sum of all adhered cell contact layers. The corresponding effective mass density is $EMD = m_{PLL} + N(t)m_c$, where *N(t)* is the number of cells having adhered to QCM surface over time (*t*). Essentially, EMD represents the extent of coverage of RBCs adherent to the PLL layer as they flow through the chamber and is dependent on RBC count. Meanwhile, the real part of the complex shear modulus of the viscoelastic layer, effective elasticity, *EE*, is simply equal to $EE = real(G) = N(t)\mu_c$ .The respective imaginary part is defined by buffer viscosity only, $imaginary(G) = 2\pi f_{air}\eta_v$. Thus, in practical terms, as the buffer dictates the viscosity parameter of G, which is defined at the start of the experiment and is constant throughout, then it has little influence on the elasticity parameter, which is dominated by the viscoelasticity of the RBC layer, as represented by *EE*. Eq.1 can be solved in terms of $\eta_v$ at $t < 0$ i.e. before the RBC suspension is loaded to the measurement chamber where $N(t) = 0$, in a form:

$$\eta_v = \Delta\Gamma^2(0)/\pi f_{air}\rho C^2 \quad (2)$$

Then, at $t > 0$, eq.1 can be solved in terms of effective mass density and effective elasticity under the assumption that the density and viscosity of the viscoelastic layer is not changing during the test:

$$EMD(t: t > 0) = A\cdot\left(-\Delta f(t) - \frac{\Delta\Gamma^2(0)}{\Delta\Gamma(t)}\right) \quad (3)$$

$$EE(t: t > 0) = B\cdot\left(\Delta\Gamma^2(t) - \frac{\Delta\Gamma^4(0)}{\Delta\Gamma^2(t)}\right) \quad (4)$$

One may notice that the mass density of the PLL layer corresponds to an *EMD* value at $t = 0$, i.e. $m_{PLL} = EMD(0) = A(-\Delta f(0) - \Delta\Gamma(0))$. To make the model parameters dimensionless and more practical in use, coefficients $A = 1/2\pi f_{air}C$ and $B = 1/\rho C$ are replaced by the values normalised against PBS, namely $A = 1/\Delta\Gamma(0)$ and $B = 1/\Delta\Gamma 2(0)$. Both *EMD* and *EE* values directly depend on the number of adhered cells, *N(t)*, and increase continuously over the course of time until they reach saturation. *N(t)* in general is unknown and another parameter, rigidity factor (RF), is introduced:

$$RF(t: t > 0) = \frac{\mu_c}{m_c} = \frac{EE(t)}{EMD(t) - EMD(0)} \quad (5)$$

which is independent of both time and cell number. The *RF* can be measured by monitoring the evolution of *EE* and *EMD* over time. By accounting for the mass of RBCs deposited (*EMD*) and the corresponding viscoelastic parameter (*EE*), the single parameter relating to RBC rigidity (deformability), *RF*, can be obtained.

### 3. Results and discussion

Fig. 3 is a coplanar analysis of the raw data (-$\Delta f$ vs.$\Delta\Gamma$) from Fig.1 and the model parameters (*EMD* vs. *EE*). A convenient way to interpret the (-$\Delta f$ vs.$\Delta\Gamma$) plots is to supplement the actual curve with a theoretical "Newtonian layer" line (-$d\Delta f/d\Delta\Gamma=1$) representing a suspension of purely viscous particles adhered to the sensor surface [23, 29]. A slope <1 would be an indication of layer viscoelasticity where the elastic properties of the particles dominate over viscosity, and a slope >1 would be associated with a formation of a firmly surface-coupled mass layer (similarly to what was observed during PLL solution in-flow). One can see that the rigid cell curve is dramatically shifted towards elevated elasticity effect. The "mass-spring" model mentioned above can further aid in the quantification of this phenomenon. First, one can see that the model is able to linearize the problem of data interpretation. *EMD* is a quasi-linear function of *EE* where its intercept corresponds to the PLL layer rigid mass density and its slope is the rigidity factor, *RF*. As was expected, the *RF* does not change over time since it is an intrinsic property of each cell and effectively represents a population average. The reduced membrane flexibility caused by the cross-linking of the RBCs with glutaraldehyde essentially makes the cells more elastic and less deformable, which is quantified by *RF*.

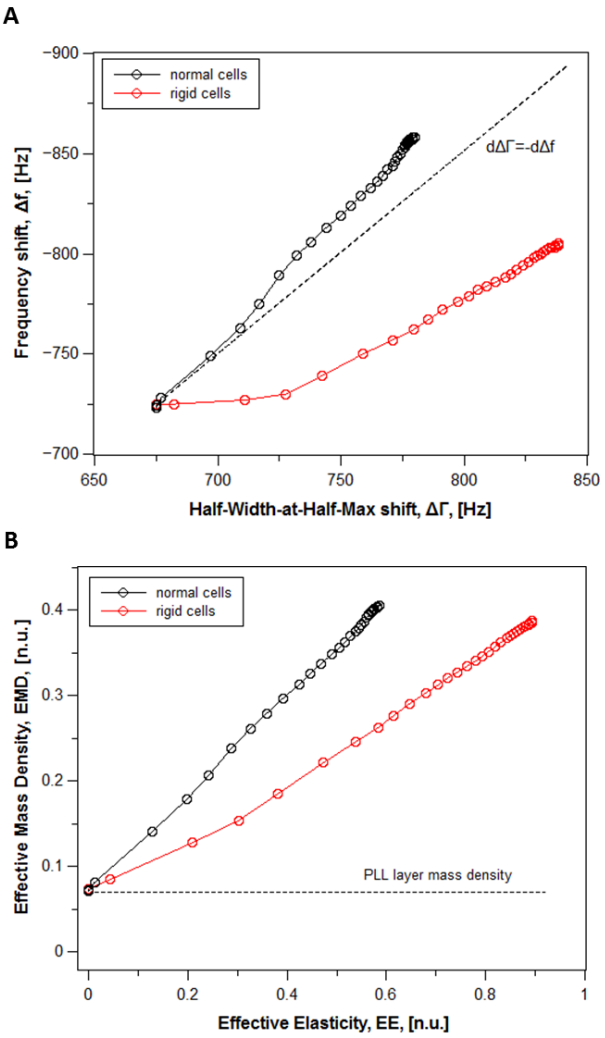


**Fig.3.** Phase plane analysis for (a) raw data recorded during the tests presented on Fig.1 for *t>0* and; (b) for the model parameters Effective Mass Density (*EMD*) and Effective Elasticity (*EE*). Time interval between points is equal to 30 s.

Another interesting observation is the approximate equality of the final *EMD* values for the suspensions of normal and rigidized cells. The latter can be interpreted as the equal number of cells having been finally accumulated on the surface and is an extrinsic property dependent on cell numbers and sedimentation rates. *EMD* effectively acts as a measure of total RBC numbers, and when used in conjunction with *EE*, demonstrates that *RF* can be measured without being affected by RBC numbers. While variations in mean corpuscular volume may not affect mass density, it would alter the inferred relationship between EMD and cell number. The manner in which the

model linearizes the effect of elevated elasticity in combination with the simplicity with which the assay can be performed provides a promising basis for the development of robust point-of-care diagnostic methods of RBC deformability. To illustrate this, a set of five samples (taken from a cohort of normal individuals) were compared in terms of their normal and artificially rigidized state, and in which unmodified cell suspensions were prepared at 1:100 and 1:10 dilutions in PBS, while the rigidized cells were prepared at 1:10 dilution only (Fig. 4). Firstly, the higher dilution did result in a predictable decrease in *EMD* shift, since there were fewer cells to accumulate on the QCM surface.

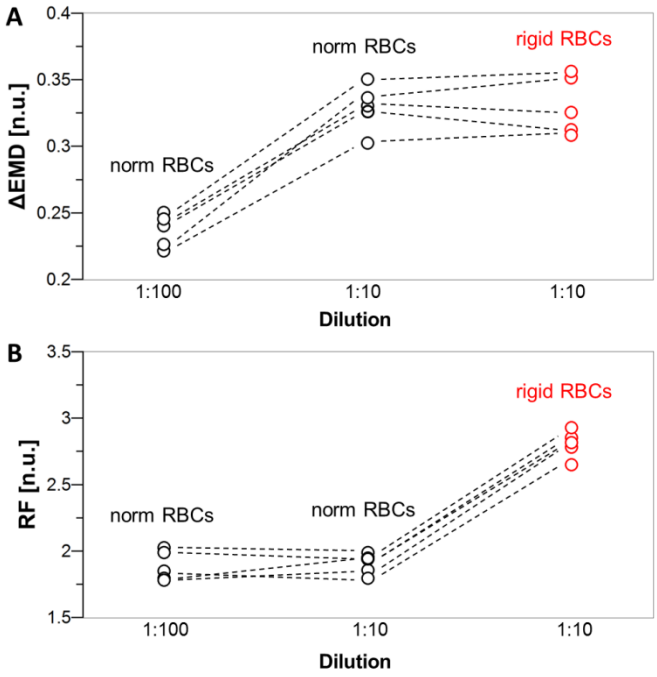


**Fig. 4**. Model output parameters of: A - Effective Mass Density (*EMD*) shift, and B - Rigidity Factor (*RF*) of five normal (black) and rigidised (red) RBC samples at dilutions of 1:10 and 1:100 in PBS.

However, the rigidity factor remained at approximately the same level, and was largely independent of a ten-fold difference in RBC count. In addition, RBC count can vary significantly between normal individuals (4.7 to 6.1 x $10^6$ per µl), which was not taken into account during cell suspension preparation. However, the obtained results confirm that the *RF* value is independent of RBC count.

Secondly, the *EMD* values for all five samples at 1:10 dilution were within a very narrow range, and the final corresponding *RF* value is a strong indicator of elevated RBC elasticity, and therefore decreased deformability.

## 4. Conclusions

A viscoelastic measurement method based on QCM and a novel mathematical model was shown to differentiate reliably between normal RBCs and those that had been artificially rigidized in a manner consistent with a pathological state. The test, which required approximately 300 µl of sample, employed modification of the QCM surface with a layer of poly-L-lysine for effective cell capture and increased sensitivity. The mathematical model allowed effective quantification of elevated RBC elasticity through the introduction of a “Rigidity Factor” parameter. The assay was sensitive to changes in RBC rigidity of three-to-four fold; levels which are typically encountered in sickle-cell disease. While Effective Mass Density and Effective Elasticity were individually sensitive to RBC concentration, the Rigidity Factor parameter was not and was capable of the concentration-independent measurement of the deformability of RBC populations. This, combined with the technical simplicity of the method creates a promising foundation for the development of convenient point-of-care methods for measurement of RBC deformability.

## Acknowledgement

This material is based on work supported by Science Foundation Ireland, Grant No.10/CE/B1821.

## References

[1] A. Bransky, N. Korin, Y. Nemirovski, U. Dinnar, An automated cell analysis sensing system based on a microfabricated rheoscope for the study of red blood cells physiology, Biosens. Bioelectr. 22 (2006) 165–169.

[2] A.G. Moutzouri, A.T. Skoutelis, C.A. Gogos, Y.F. Missirlis, G.M. Athanassiou, Red blood cell deformability in patients with sepsis: a marker for prognosis and monitoring of severity, Clin. Hemorheol. Microcirc. 36 (2007) 291–299.

[3] K. Donadello, M. Piagnerelli, G. Reggiori, L. Gottin, S. Scolletta, G. Occhipinti, K. Zouaoui Boudjeltia, J.L. Vincent, Reduced red blood cell deformability over time is associated with a poor outcome in septic patients, Microvasc. Res. 101 (2015) 8–14.

[4] S.K. Ballas, E.D. Smith, Red blood cell changes during the evolution of the sickle cell painful crisis, Blood 79 (1992) 2154–2163.

[5] Y. Alapan, J.A. Little, U.A. Gurkan, Heterogeneous red blood cell adhesion and deformability in sickle cell disease, Sci. Rep. 4 (2014) 7173.

[6] A.M. Dondorp, P.A. Kager, J. Vreeken, N.J. White, Abnormal blood flow and red blood cell deformability in severe malaria, Parasitol. Today 16 (2000) 228–232.

[7] C.D. Brown, H.S. Ghali, Z. Zhao, L.L. Thomas, E.A. Friedman, Association of reduced red blood cell deformability and diabetic nephropathy, Kidney Int. 67 (2005) 295–300.

[8] A. Goldin, J.A. Beckman, A.M. Schmidt, M.A. Creager, Advanced glycation end products: Sparking the development of diabetic vascular injury, Circulation 114 (2006) 597–605.

[9] Y. Kim, K. Kim, Y-K. Park, Measurement techniques for red blood cell deformability: recent advances, in: T.E. Moschandreou (Ed.), Blood Cell - An Overview of Studies in Hematology, Rijeka: InTech, 2012, pp. 167-94.

[10] J. Kim, H.Y. Lee, S. Shin, Advances in the measurement of red blood cell deformability: a brief review, J. Cell. Biotech. 1 (2015) 63-79.

[11] K. Engstrom, H. Meiselman, Analysis of red blood cell membrane area and volume regulation using micropipette aspiration and perfusion, Biorheology 32 (1995) 115–16.

[12] I. Dulinska, M. Targosz, W. Strojny, M. Lekka, P. Czuba, W. Balwierz, M. Szymonski, Stiffness of normal and pathological erythrocytes studied by means of atomic force microscopy, J. Biochem. Biophys. Meth. 66 (2006) 1-11.

[13] I.M. Lamzin, R.M. Khayrullin, The quality assessment of stored red blood cells probed using atomic-force microscopy, Anatomy Res. Int. 2014 (2014) 869683.

[14] J. Guck, R. Ananthakrishnan, H. Mahmood, T.J. Moon, C.C. Cunningham, J. Käs, The optical stretcher: a novel laser tool to micromanipulate cells, Biophys. J. 81 (2001) 767-784.

[15] Y.K. Park, C.A. Best, K. Badizadegan, R.R. Dasari, M.S. Feld, T. Kuriabova, M.L. Henle, A.J. Levine, G. Popescu, Measurement of red blood cell mechanics during morphological changes, Proc. Nat. Acad. Sci. 107 (2010) 6731.

[16] M. Srour, Y. Bilto, M. Juma, M.R. Irhimeh, Exposure of human erythrocytes to oxygen radicals causes loss of deformability, increased osmotic fragility, lipid peroxidation and protein degradation, Clin. Haemorheol. Mircocirc. 23 (2000) 13-22.

[17] H. Bow, I.V. Pivkin, M. Diez-Silva, S.J. Goldfless, M. Dao, J.C. Niles, S. Suresh, J. Han, A microfabricated deformability-based flow cytometer with application to malaria, Lab on a Chip, 11 (2011) 1065-73.

[18] 18.R.M. Johnson, Ektacytometry of red blood cells, Meth. in Enzym. 173 (1989) 35-54.

[19] S. Zhang, H. Bai, P. Yang, Real-time monitoring of mechanical changes during dynamic adhesion of RBCs to endothelial cells by QCM-D, Chem. Commun. 51 (2015) 11449.

[20] M.J. Santos-Martinez, I. Inkielewicz-Stepniak, C. Medina, K. Rahme, K.M. D'Arcy, D. Fox, J.D. Holmes, H. Zhang, M.W. Radomski, The use of quartz crystal microbalance with dissipation (QCM-D) for studying nanoparticle-induced platelet aggregation, Int. J. Nanomed. 7 (2012) 243–255.

[21] H.L. Bandey, R.W. Cernosek, W.E. Lee, L.E. Ondrovic, Blood rheological characterization using the thickness-shear mode resonator, Biosens. Bioelectr. 19 (2004) 1657-1665.

[22] M.V. Voinova, M. Jonson, B. Kasemo, Missing mass effect in biosensor's QCM applications, Biosens. Bioelectr. 17 (2002) 835-41.

[23] V. Efremov, R.S. Lakshmanan, B. Byrne, S. M. Cullen, A.J. Killard, Modelling of blood component flexibility using quartz crystal microbalance, J. Biorheol. 28 (2014) 45–54.

[24] I. Shock, A. Barbul, P. Girshovitz, U. Nevo, R. Korenstein, N.T. Shaked, Optical phase nanoscopy in red blood cells using low-coherence spectroscopy, J. Biom. Opt. 17(2012) 101509-1-5.

[25] J.L. Maciaszek, B. Andemariam, G. Lykotrafitis, Microelasticity of red blood cells in sickle cell disease, The J. Strain Anal. Eng. Des. 46 (2011) 368-379.

[26] C. Brezinski, Rational approximations to formal power series, J. Approx. Theory 25 (19790 295–317.

[27] V. Efremov, A.J. Killard, B. Byrne, R.S. Lakshmanan, The modelling of blood coagulation using the quartz crystal microbalance, J. Biomech 46 (2013) 437–42.
[28] D. Johannsmann, Studies of Viscoelasticity with the QCM, in: A. Janshoff, C. Steinem (Eds.), Piezoelectric Sensors, Springer-Verlag Berlin Heidelberg, 2007, pp. 49-109.
[29] L. Müller, S. Sinn, H. Drechsel, C. Ziegler, H.P. Wendel, H. Northoff, F.K. Gehring, Investigation of Prothrombin Time in Human Whole-Blood Samples with a Quartz Crystal Biosensor, Anal. Chem. 82 (2010) 658–663.